The Spatial Model of Flood Risk in the Kanjiro River Basin, North Luwu District, Indonesia

Mukhsan Putra Hatta
Department of Civil Engineering, Hasanuddin University, Makassar, Indonesia
mukhsan.hatta@unhas.ac.id (corresponding author)

Silman Pongmanda
Department of Civil Engineering, Hasanuddin University, Makassar, Indonesia
silmanpongmanda@unhas.ac.id

Ariningsih Suprapti
Department of Civil Engineering, Hasanuddin University, Makassar, Indonesia
ariningsihsuprapti@unhas.ac.id

Kartika Sari
Department of Civil Engineering, Hasanuddin University, Makassar, Indonesia
kartikasari@unhas.ac.id

Syamsu Rijal
Faculty of Forestry, Hasanuddin University, Makassar, Indonesia
syamsurijal@unhas.ac.id

Wasir Samad
Faculty of Mathematics and Science, Hasanuddin University, Makassar, Indonesia
wasirsamad@unhas.ac.id

Fery Fadlin
State Agricultural Polytechnic, Samarinda, Indonesia
ferifadlin@gmail.com

Received: 14 January 2025 | Revised: 16 February 2025 | Accepted: 6 March 2025

DOI: https://doi.org/10.48084/etasr.10235

ABSTRACT

Flood risk mitigation in North Luwu Regency faces challenges due to the lack of detailed spatial data on the region's complex topography. This limitation increases the potential for material and non-material losses. Accurate flood-prone area mapping requires reliable topographical and elevation data, which can be effectively obtained through Unmanned Aerial Vehicles (UAVs). The UAV technology enables high-resolution spatial data collection over large areas quickly and efficiently. This study integrates UAV surveys with terrestrial and hydrographic (bathymetric) measurements to develop a comprehensive flood risk spatial model. The objectives include the evaluation of the accuracy of the integrated rapid survey method and the design of a spatial model for flood risk reduction in the Kanjiro River Basin, North Luwu Regency. The study results include a high-resolution flood risk spatial model, structural and non-structural flood mitigation strategies, and a two-dimensional flood simulation using the HEC-RAS numerical model. The simulation assesses flood propagation, depth, and velocity, validated through primary data measurements. The findings provide a valuable tool for urban flood risk management and contribute to developing data-driven policies for flood mitigation.

Keywords-flood disaster; flood risk; flood control mitigation; UAV

I. INTRODUCTION

The major river basin of Pompengan-Jeneberang operational area encompasses key river basins in South Sulawesi, including the Saddang, Walanae-Cenranae, and Pompengan Larona river. These river basins are expected to experience significant development due to their extensive geographical coverage and high potential for natural resource utilization. However, these regions also face critical environmental challenges, such as flooding, drought, and landslides, which pose risks to both infrastructure and communities.

To mitigate these hazards, various river infrastructure projects have been developed, alongside operational and maintenance efforts aimed at ensuring sustainable functionality of flood control measures. One essential aspect of flood and landslide mitigation planning is the development of flood vulnerability maps, which serve as crucial tools for disaster risk management and land-use planning. Mapping flood-prone areas enhances the ability to predict and manage flood risks by identifying high-risk zones and formulating appropriate mitigation strategies [1]. A key component of river management is the concept of river inventory, which involves assessing and restoring functions, such as ecological connectivity, irrigation, and drainage. This concept represents an evolution from traditional river development approaches, emphasizing a balance between human benefits and environmental conservation. The eco-hydraulic approach, which integrates ecological considerations into hydraulic engineering, is increasingly recognized as a vital strategy for sustainable water resource management.

In Indonesia, effective river management necessitates a shift toward a more ecologically informed and integrated approach. The creation of inventory maps for flood-prone areas should be conducted systematically, beginning with smaller rivers and extending to larger water bodies. This process requires a comprehensive understanding of both biotic and abiotic factors influencing river dynamics. Additionally, strategies, such as increasing river retention areas, collecting infrastructure data, enhancing the resilience of natural flood banks, and employing eco-engineering techniques for river restoration, contribute to the overall improvement of flood mitigation efforts [2, 3].Failure to maintain accurate and up-to-date river database inventories can result in severe consequences, including unintended land use for residential, industrial, or agricultural purposes. The rectification of altered river courses is costly, involving land acquisition expenses and intensive sediment management due to rapid erosion and deposition processes. Straightened river sections are particularly susceptible to accelerated erosion, while downstream channels may experience heightened sedimentation, further complicating flood management efforts [4]. Despite the existing research and infrastructure efforts, significant gaps remain in the understanding and application of flood risk modeling and mitigation strategies in Indonesia. Current studies often lack a comprehensive integration of remote sensing technology, hydrodynamic modeling, and ecological assessments in flood risk analysis. Therefore, this research aims to address these gaps by developing a spatial model for flood risk assessment in the Kanjiro River Basin, North Luwu Regency. It integrates advanced geospatial techniques, including UAV-based topographic surveys and hydrodynamic simulations, to enhance the accuracy and reliability of flood vulnerability mapping. The findings will contribute to improving flood risk reduction strategies, informing policy decisions, and supporting sustainable river management initiatives in Indonesia.

II. LITERATURE REVIEW

A. *Unmanned Aircraft Technology*

Nowadays, there is a tremendous development in mapping technology, with one of the main advancements being the increased usage of UAVs, also referred to as unmanned aircraft. This research deploys the UAV technology to gather data regarding the topography and land cover of the river region under study. High-resolution mapping rules utilized in UAV technology are followed during the data gathering procedure, which includes the following steps [5, 6]:

- Determination of take-off location (identification of obstacles and take-off/landing position).
- Determination and installation of Ground Control Points (GCP) and Independent Control Points (ICP).
- Determination of height and flight path.
- Execution of flight missions.
- Quality checking and image processing (Orthophoto, Point Cloud, DSM/DTM).
- GIS analysis for land cover and topography data extraction.

Installing ground GCPs at various locations that correspond to the study site is one of the procedures in the UAV data collection process. The coordinates (X, Y) and altitude values (Z) of the GCPs were measured using geodetic GPS in accordance with the Real Time Kinematic (RTK) technique. The closest geodetic control point or Continuously Operating Reference Station (CORS) station to the study site serves as the base. GCP is applied to enhance the geometric accuracy of UAV-taken images. The Geospatial Information Agency (BIG) Number 15 of 2014's Technical Guidelines for Base Map Accuracy serves as the basis for testing geometric accuracy.

B. *State of The Art*

Numerous studies deal with spatial flood modeling, employing a range of techniques and strategies. Using Geographic Information Systems to map flood zones and create hydrodynamic models is one of the most impressive works. Echosounder technology is used in this study to map the bathymetry of rivers. The study's findings include a terrain model that simulates flood zones by combining river bathymetry and land topography data (30-meter spatial resolution DEM). Flood risk was also mapped using a combination of remote sensing and Geographic Information Systems (GIS) in the downstream regions of the Togo River, West Africa. A flood risk map is the primary product of this study, which uses the DAS (River Watershed) as its analytical unit [7-10]. Using administrative regions as the unit of analysis, research on flood risk assessment employing LiDAR technology was conducted in [5]. This study's primary goal was to increase the basic data's accuracy for the modeling of flood areas.

III. METHODOLOGY

A. Research Location

The Kanjiro watershed in North Luwu Regency is where this study was carried out. While there are many areas within the administrative boundaries of North Luwu Regency, this study will concentrate mostly on areas that are vulnerable to flooding, particularly in Somba Opu District. The research location is shown in Figure 1, and the data as well as the information utilized in this study were taken from the findings of earlier investigations [5].

B. Research Methods

The conduct of this research included three phases: planning, gathering and analyzing data, and writing the report. Table I contains specifics on each step of the research methodology.

TABLE I. RESEARCH METHODS

Research purposes	**Data components**	**Data collection and analysis procedures**	**Outcome targets/Achievement indicators**
Utilize hydrographic, terrestrial, and aerial photo survey techniques to swiftly and comprehensively gather data and information on flood-prone locations. Then, verify the accuracy of the resultant data.	Secondary data Administrative limits Areas prone to flooding Existing drainage System map Daily rainfall and measured discharge (if any) Land use Length and slope of land/river Primary data Bathymetry of rivers/secondary and primary drainage channels River/drainage geometry and, Topography Aerial photo of flood prone areas	Secondary Data The preparation stage includes collecting Indonesian Earth Maps, Digital Elevation Models (DEM), and rainfall The data processing/analysis stage includes making administrative maps, watershed and CA boundaries of the study location, land use and slope, as well as river length and slope using ArcGis Pro 2.6 software, rainfall analysis and return period design flood discharge calculations. Primary data The preparation stage includes providing equipment (Echosounder) and ships as measurement vehicles, providing UAVs, installing stakes and measuring GCP coordinates, as well as preparing flight routes for aerial photo surveys. The data processing/analysis stages include processing bathymetric data using Microsoft Excel and Quantum GIS as well as processing aerial photos using Agisoft Photoscan software and testing the geometric accuracy of UAV aerial photos.	North Luwu Regency design flood discharge data. Map of administrative boundaries, CA, drainage system, land use, land slope, bathymetry and topography of the area. Aerial photo of the study location. Geometric accuracy level of UAV results.
General Objective: Create spatial models and plans for structural and non-structural flood risk reduction for the North Luwu Regency area based on survey results and field data collecting. Special purpose: Evaluating the risk, susceptibility, and ability to mitigate flood risk in North Luwu Regency	Secondary Data Design flood discharge Topographic Survey Results Primary data River geometry (Topography and Bathymetry) from UAV Aerial photography from UAV	Secondary Data The preparation stage includes collecting the results of the design and flood discharge analysis. The data processing and analysis stage includes processing the design flood discharge data in Microsoft Excel Primary Data. The preparation stage includes equalizing vertical and horizontal datums as well as integrating bathymetric data, topography, and UAV photos. The data processing and analysis stage includes inputting integrated topography and bathymetry data as well as aerial photos into the Hec-Ras software to prepare a 2-dimensional flood inundation simulation.	Flood inundation spatial model based on inundation depth
Design and analyse a spatial model of flood risk in North Luwu Regency.	Secondary Data Data components of physical vulnerability, socio-economic, land use, Regional capacity in reducing flood risk Primary data Spatial model of flood depth Spatial model of flood flow velocity	Secondary data The preparation stage includes determining vulnerability components and collecting data from various sources. Data processing and analysis includes conversion of tabular data on vulnerability components into spatial data as well as classification of vulnerability components into 3 vulnerability level classes. Primary data The preparation stage includes collecting data on flood hazard components (depth and current speed). The data processing and analysis stage includes classification of depth levels and current speeds into 3 classes of flood hazard levels.	Flood danger level map Flood vulnerability level map Flood risk level map (R = H x V: C)
Provide suggestions for methods to lessen the risk of flooding in the North Luwu Regency.	Flood simulation/inundation spatial model Topography Map of flood risk levels	Analysis of determining flood risk reduction strategies	North Luwu Regency flood risk Reduction strategy Protective strategy Accommodation strategy Fallback strategy

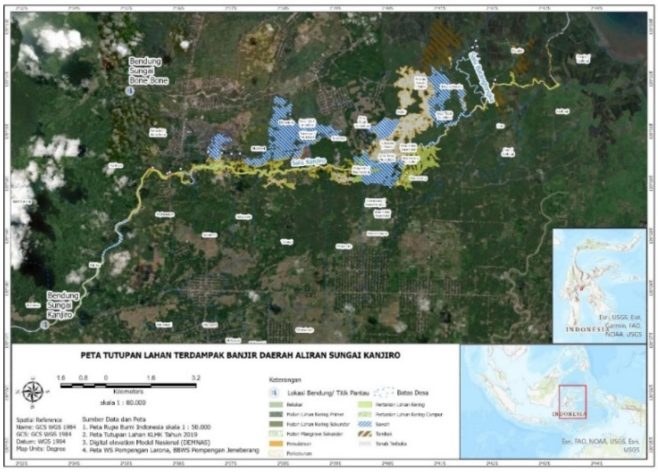

Fig. 1. Research location map.

IV. RESULTS AND DISCUSSION

A. Flood Height Inventory and Analysis

The process of choosing a reference point to serve as a coordinate base in a universal coordinate system, with a particular emphasis on geodetic height, is known as reference point binding. The locations of these geodetic high points are often those that are closest to the measuring area. Nevertheless, when conducting field searches, the team discovered that the Tide Gauge (TG) devices or pillars matching the specified code were no longer present in the field.

The closest CORS station, which is situated in Palopo City, is utilized to obtain an elevation reference. In order to gather the measurement data, using Geodetic GPS and the RTK method, the following steps were executed:

- A GPS was mounted either on the TG itself or at a connected point (transfer point).
- In order to obtain the coordinates of points (N, E, and Z) in flood-prone locations, the GPS Rover is mounted atop a pole.

Numerous pieces of information on past flood heights were gathered via field surveys and interviews considering the period 2021–2022, as shown in Table II.

TABLE II. KANJIRO WATERSHED FLOOD HEIGHT INVENTORY

No	X	Y	Location	Elevation	Depth	Duration
1	222569.94	9713251.78	District Bone-Bone, Patoloan Village	24.419	0.310	6 hours
2	222368.68	9712731.84	District Bone-Bone, Patoloan Village	26.559	0.650	1 day
3	222406.97	9712653.11	District Bone-Bone, Patoloan Village	25.334	0.470	12 hours
4	222521.19	9712265.08	District Bone-Bone, Patoloan Village	21.246	0.420	12 hours
5	226796.26	9706273.59	District Bone-Bone, Tamuku Village	4.203	0.550	1 day
6	226925.29	9706131.42	District Bone-Bone, Tamuku Village	5.252	0.750	1 day
7	226727.34	9706202.55	District Bone-Bone, Tamuku Village	3.960	1.190	1 day
8	226995.15	9706053.38	District Bone-Bone, Tamuku Village	4.828	0.840	1 day
9	226734.01	9706259.76	District Bone-Bone, Tamuku Village	2.281	0.910	1 day
10	227060.40	9706008.35	District Bone-Bone, Tamuku Village	5.481	0.830	1 day
11	227130.64	9705956.30	District Bone-Bone, Tamuku Village	4.638	1.240	1 day
12	226533.75	9706671.98	District Bone-Bone, Tamuku Village	18.640	0.340	12 hours
13	226391.32	9706939.68	District Bone-Bone, Tamuku Village	17.579	0.490	12 hours
14	225992.10	9707083.68	District Bone-Bone, Tamuku Village	18.349	0.560	12 hours
15	225843.05	9707154.94	District Bone-Bone, Tamuku Village	14.464	0.380	12 hours
16	225623.52	9707404.97	District Bone-Bone, Tamuku Village	14.975	0.830	12 hours
17	226891.85	9701817.95	District Bone-Bone, Batang Tongka Village	1.507	1.340	1 day
18	226852.98	9701980.37	District Bone-Bone, Batang Tongka Village	2.542	0.730	12 hours
19	227087.79	9701865.46	District Bone-Bone, Batang Tongka Village	2.419	1.270	12 hours
20	226627.94	9701814.85	District Bone-Bone, Batang Tongka Village	2.399	1.030	12 hours
21	226447.21	9701736.72	District Bone-Bone, Batang Tongka Village	1.877	0.890	12 hours
22	225572.04	9701230.20	District Bone-Bone, Pongko Village	4.083	0.630	12 hours
23	225709.02	9701185.01	District Bone-Bone, Pongko Village	6.617	0.420	12 hours

B. Inventory and Analysis of Flood Prone Areas

The areas impacted by flooding must be identified through an analysis using data on land use patterns that have been corroborated by field survey findings. The information below relates to the patterns of land use in each of the watersheds depicted in Figure 2. The results, outlined in Table III, made possible the determination of the area of each type of land that has been impacted by flooding.

C. Survey and Analysis Topographic Data

The creation of flood prone area maps for the Pompengan, Balease, Kanjiro, Bone-Bone, Bunga Didi, and Battang watersheds, as well as the primary element of the 2D numerical model simulation process, are both heavily dependent on topographic survey activities. These activities have a significant impact on the areas that experience flooding.

The Indonesian Geospatial Information Agency's National Horizontal Control Net (JKHN) and National Vertical Control

Net (JKVN) provide the vertical and horizontal reference data needed for topographic surveys. The geodetic control data used in this study are sourced from the Palopo City CORS station, which is the closest one.

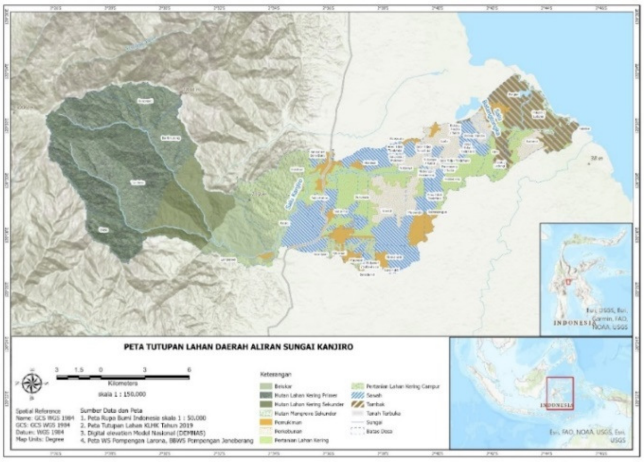

Fig. 2. Kanjiro Watershed Land Cover.

TABLE III. KANJIRO WATERSHED FLOOD AFFECTED AREAS.

Land use	Area (Hectares)
Body of water	88.22
Thicket	3.84
Secondary mangrove forest	2.94
Settlement	10.47
Plantation	358.33
Dry land farming	282.85
Mixed dry land agriculture	14.61
Rice field	304.77
Pond	1018.35
Open land	0.16

To determine which geodetic response point (TG) will be used, based on the data and the geodetic control description, the shortest path between the TG and the topographic measurement location was considered, as well as the physical conditions surrounding the TG. These conditions are intended to be open in order to maximize the accuracy of both static and RTK methods for capturing satellite signals during measurements, including surface height (BM) and CP.

A theodolite and/or total station with a maximum accuracy of 2", and a water pass with an accuracy of 1 mm and a magnification of 32 times are among the required parameters for the survey's instruments. With the exception of river measurements, topographic data will be integrated with the Digital Elevation Model (DEM) and the Digital Surface Model (DSM), which are produced using drone data.

The overall goal of this endeavor is to gather topographic data that will serve as foundational information for 2D numerical simulations using the HEC-RAS program. Table IV provides topographic measuring data for each river [11, 12].

TABLE IV. DATA FROM TOPOGRAPHIC MEASUREMENTS OF THE KANJIRO WATERSHED.

No	X	Y	Z
1	222569.94	9713251.78	28.10
2	222368.68	9712731.84	26.30
3	222406.97	9712653.11	26.80
4	222521.19	9712265.08	26.10
5	226796.26	9706273.59	7.88
6	226925.29	9706131.42	7.43
7	226727.34	9706202.55	8.14
8	226995.15	9706053.38	7.52
9	226734.01	9706259.76	8.07
10	227060.40	9706008.35	6.92
11	227130.64	9705956.30	6.53
12	226533.75	9706671.98	1.30
13	226391.32	9706939.68	9.95
14	225992.10	9707083.68	11.31
15	225843.05	9707154.94	11.58
16	225623.52	9707404.97	13.92
17	226891.85	9701817.95	9.51
18	226852.98	9701980.37	9.93
19	227087.79	9701865.46	8.51
20	226627.94	9701814.85	7.74
21	226447.21	9701736.72	6.14
22	225572.04	9701230.20	7.98
23	225709.02	9701185.01	8.03

D. Map of Kanjiro Watershed Flood Prone Areas

The Kanjiro watershed's flood discharge predictions were created through modeling with HEC-HMS and the results are presented in Table V. Figure 3 shows the hydrographic graph of the flood discharge in the area.

TABLE V. WATERSHED DESIGN FLOOD

Return time (years)	Kanjiro dam DTA flood discharge (m^3/s)	Suspension bridge DTA flood discharge (m^3/s)
2	85.2	156.6
5	161.4	276.6
10	216.8	363
25	290.4	477.2
50	346.8	564.2
100	404	653

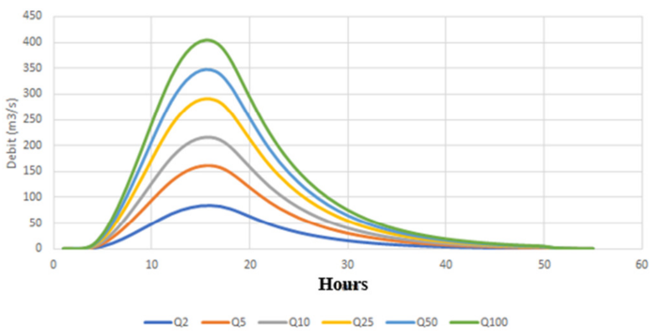

Fig. 3. Flood discharge in the Kanjiro Dam catchment area.

E. Overflow Point on a River Bank in the Kanjiro Watershed

According to BNPB standards from 2012, the flood risk levels are categorized based on the water depth. Water depths less than 0.76 m are classified as low risk levels, water depths between 0.76 and 1.5 m as medium risk levels, and water depths greater than 1.5 m as high-risk levels, as depicted in Table VI [13].

TABLE VI. Q25 FLOOD INUNDATION AREA BASED ON KANJIRO WATERSHED ADMINISTRATION.

No.	Village	Classification		
		Low	Currently	High
1	Sukaraya	49.59 (Ha)	36.86 (Ha)	48.42 (Ha)
2	Sadar	42.14	51.85	215.65
3	Pongko	35.05	12.73	16.45
4	Muktisari	122.80	88.77	48.08
5	Batang Tongka	64.12	54.39	102.11
6	Banyuurip	43.59	9.94	1.04
7	Tolangi	23.41	11.05	4.10
8	Sukamaju	1.31	0.81	13.44
9	Rawamangun	4.10	5.11	81.55
10	Paomacang	50.59	47.25	2.26

The next step is to overlay land use pattern data, as depicted in Table VIII, with flood area maps, as displayed in Figures 4-7, to determine the affected area of each type of land. Furthermore, information about the land use patterns that have been confirmed by field surveys is required to pinpoint the locations impacted by flooding, as can be seen in Table VII.

TABLE VII. OVERFLOW POINT ON A RIVER BANK IN THE KANJIRO WATERSHED.

No.	X	Y	Village	Sub District	District
1	225718.83	9700485.74	Pongko	Bone Bone	North Luwu
2	225217.02	9701337.29	Lino	Sukamaju	
3	224547.95	9702264.87	Batang Tongka	Bone Bone	
4	222844.84	9705199.68	Sukaraya	Bone Bone	
5	222647.16	9706203.29	Sukaraya	Bone Bone	
6	222586.34	9706963.61	Tolangi	Sukamaju	
7	222449.48	9707723.92	Tolangi	Sukamaju	
8	222571.13	9708864.39	Muktisari	Bone Bone	
9	222525.51	9709046.87	Muktisari	Bone Bone	
10	222160.56	9709092.49	Tolangi	Sukamaju	
11	222343.04	9709381.40	Sukamaju	Sukamaju	
12	222464.69	9709898.42	Muktisari	Bone Bone	
13	222479.89	9710232.96	Muktisari	Bone Bone	
14	222647.16	9710461.05	Muktisari	Bone Bone	
15	222434.27	9711054.09	Salulemo	Sukamaju	
16	222631.96	9711175.74	Muktisari	Bone Bone	
17	222647.16	9711814.41	Patoloan	Bone Bone	
18	222343.04	9712270.60	Saptamarga	Sukamaju	
19	222373.45	9712301.01	Saptamarga	Sukamaju	

TABLE VIII. SIZE OF FLOODED AREA

Land use pattern	Inundation area (Ha)			Total (Ha)
	< 0.76 m	0.76 - 1.5 m	> 1.5 m	
Open land	0.08	0.00	0.00	0.08
Plantation/Garden	84.64	85.16	188.52	358.33
Places of activity	3.91	3.10	3.06	10.07
Ricefield	69.51	56.18	179.53	305.22
Shrubs	0.28	0.34	3.22	3.84
Pond	554.63	321.37	142.35	1018.3

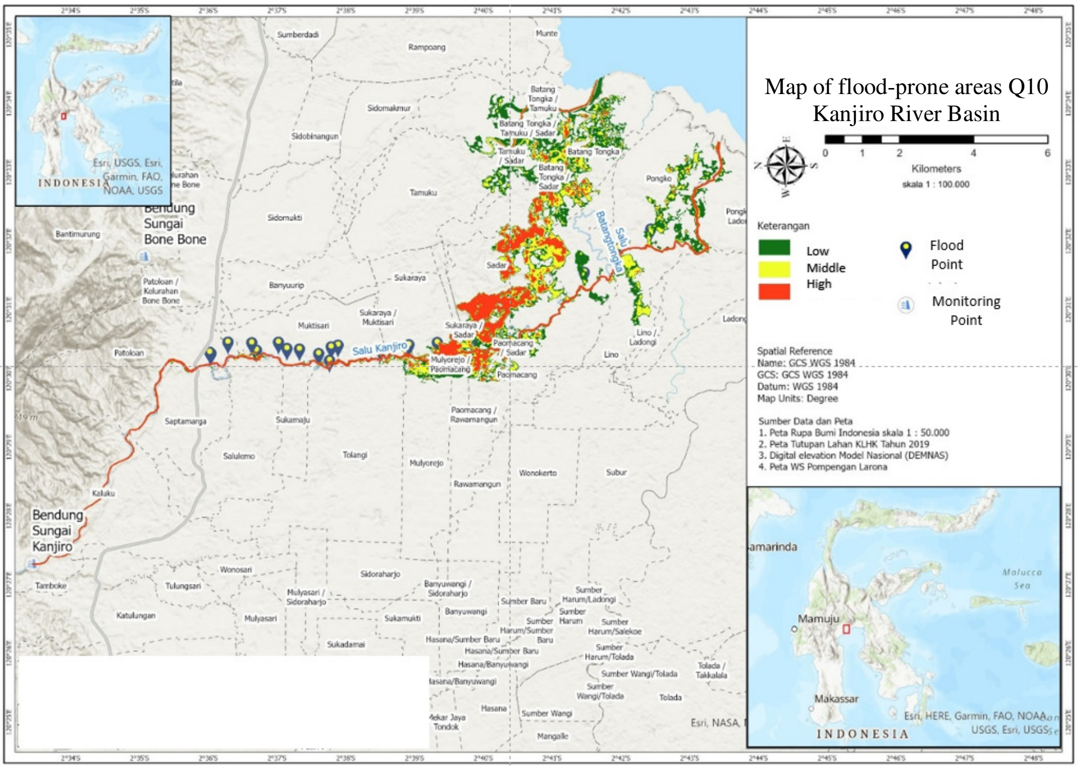

Fig. 4. Kanjiro Q10 watershed flood prone area.

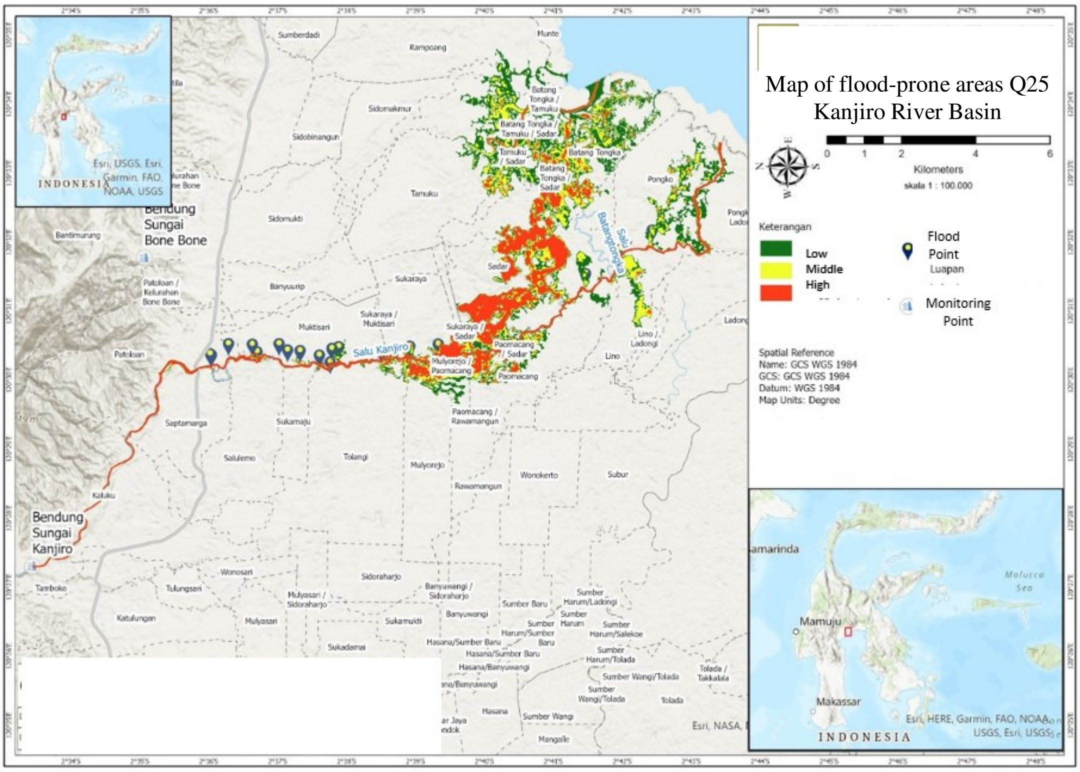

Fig. 5. Kanjiro Q25 watershed flood prone area.

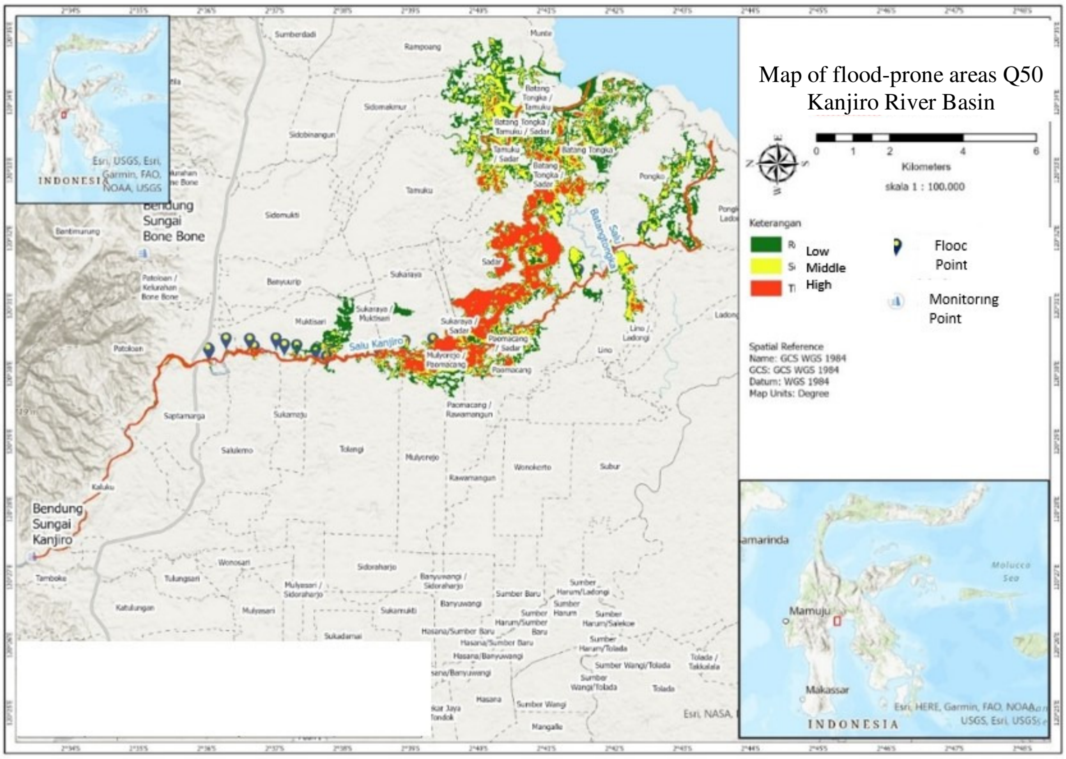

Fig. 6. Kanjiro Q50 watershed flood prone area.

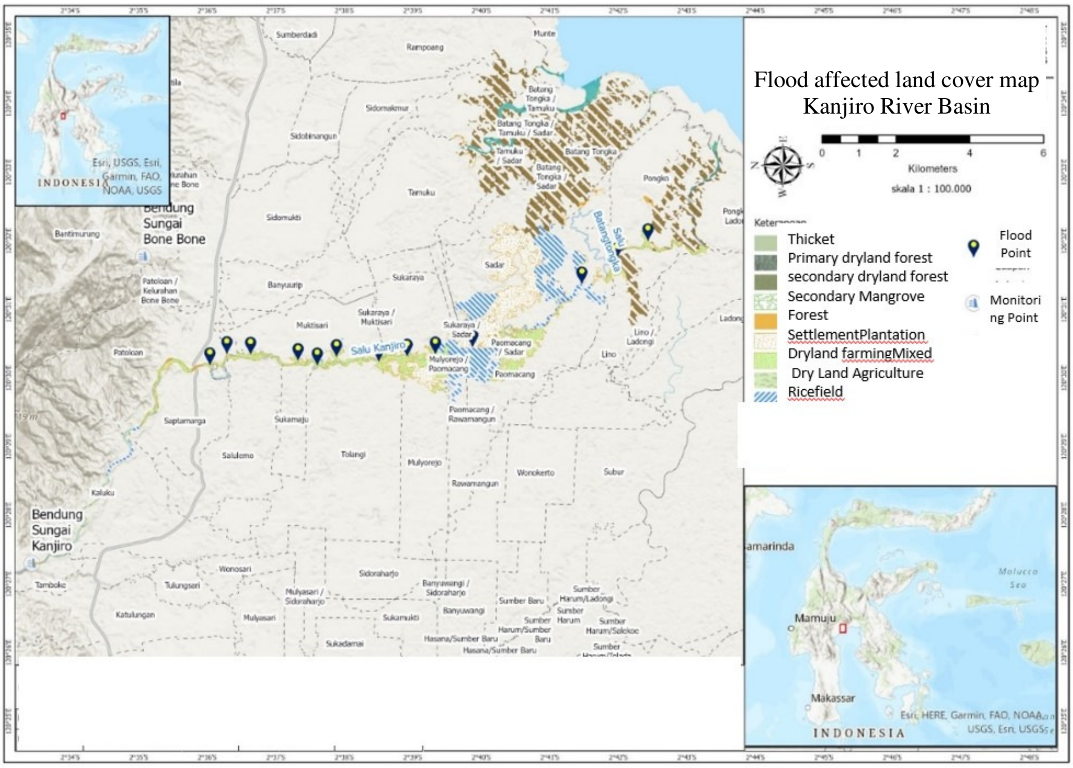

Fig. 7. Impact of flooding in the Kanjiro watershed.

V. CONLUSION

This study's goal was to address a critical knowledge gap in flood risk assessment by integrating spatial analysis with hydrological data. While previous research has explored flood hazards in various regions, limited studies have specifically focused on the Kanjiro River Basin using advanced spatial modeling techniques. This research follows a systematic approach, including data collection, spatial mapping, risk classification, and model validation. The key findings highlight the flood-prone areas, risk factors, and the influence of land use and topography on flood susceptibility. The novelty of this study lies in its application of Geographic Information Systems (GIS)-based spatial modeling tailored to the local hydrological and environmental conditions, offering a refined risk assessment tool for disaster management. Comparisons with similar studies reveal the effectiveness of this approach in enhancing predictive accuracy and guiding mitigation strategies. The results include:

- The inundation is located in two sub-districts: Sukamaju District (which includes Tolangi Village 38.56 Ha, Sukamaju Village 15.56 Ha, Rawamangun Village 90.76 Ha, and Paomacang Village 100.10 Ha) and Bone-Bone District (which includes Sukaraya Village 134.87 Ha, Sadar Village 309.64 Ha, Pongko Village 64.22 Ha, Muktisari Village 259.65 Ha, Batangtongka Village 220.62 Ha, and Village Banyuurip 54.57 Ha).
- The simulation results reveal the amount of the inundation.
- Areas with a low flood danger level (<0.76 m) cover 680.60 ha for discharge Q10, 440.28 ha for a medium flood danger level (0.76 m–1.5 m), and 497 ha for a high flood danger level (>1.5 m).
- Areas having a low flood risk level (838.14), a medium flood danger level (553.95), and a high flood hazard level (690.17 ha) are covered for discharge Q25.
- For discharge Q50, 967.29 hectares are covered by places with a low flood danger level, 670.56 ha by regions with a medium flood danger level, and 793.26 ha by areas with a high flood danger level.

REFERENCES

[1] N. Harkat, S. Chaouche, and M. Bencherif, "Flood Hazard Spatialization Applied to The City of Batna: A Methodological Approach," *Engineering, Technology & Applied Science Research*, vol. 10, no. 3, pp. 5748–5758, Jun. 2020, https://doi.org/10.48084/etasr.3429.

[2] F. Fadlin, M. A. Thaha, F. Maricar, and M. P. Hatta, "Validation of satellite-based precipitation products TRMM using ground-based measurements," *AIP Conference Proceedings*, vol. 2543, no. 1, Nov. 2022, Art. no. 030007, https://doi.org/10.1063/5.0095358.

[3] M. P. Hatta, F. Fadlin, R. Harun, Y. Elfita, and I. Renreng, "Application of 2D numerical simulation for the analysis of July 2020 North Luwu flood," *IOP Conference Series: Earth and Environmental Science*, vol. 841, no. 1, Art. no. 012028, Dec. 2021, Art. no. 012028, https://doi.org/10.1088/1755-1315/841/1/012028.

[4] C. Ben Khalfallah and S. Saidi, "Spatiotemporal floodplain mapping and prediction using HEC-RAS - GIS tools: Case of the Mejerda river, Tunisia," *Journal of African Earth Sciences*, vol. 142, pp. 44–51, Jun. 2018, https://doi.org/10.1016/j.jafrearsci.2018.03.004.

[5] V. Merwade, A. Cook, and J. Coonrod, "GIS techniques for creating river terrain models for hydrodynamic modeling and flood inundation

mapping," *Environmental Modelling & Software*, vol. 23, no. 10, pp. 1300–1311, Oct. 2008, https://doi.org/10.1016/j.envsoft.2008.03.005.

[6] R. Mind'je *et al.*, "Flood susceptibility modeling and hazard perception in Rwanda," *International Journal of Disaster Risk Reduction*, vol. 38, Aug. 2019, Art. no. 101211, https://doi.org/10.1016/j.ijdrr.2019.101211.

[7] J. Ntajal, B. L. Lamptey, I. B. Mahamadou, and B. K. Nyarko, "Flood disaster risk mapping in the Lower Mono River Basin in Togo, West Africa," *International Journal of Disaster Risk Reduction*, vol. 23, pp. 93–103, Aug. 2017, https://doi.org/10.1016/j.ijdrr.2017.03.015.

[8] X. Qiao *et al.*, "A systems approach to routing global gridded runoff through local high-resolution stream networks for flood early warning systems," *Environmental Modelling & Software*, vol. 120, Oct. 2019, Art. no. 104501, https://doi.org/10.1016/j.envsoft.2019.104501.

[9] V. M. Quirogaa, S. Kurea, K. Udoa, and A. Manoa, "Application of 2D numerical simulation for the analysis of the February 2014 Bolivian Amazonia flood: Application of the new HEC-RAS version 5," *Ribagua*, vol. 3, no. 1, pp. 25–33, Jan. 2016, https://doi.org/10.1016/j.riba.2015.12.001.

[10] M. Rusnák, J. Sládek, A. Kidová, and M. Lehotský, "Template for high-resolution river landscape mapping using UAV technology," *Measurement*, vol. 115, pp. 139–151, Feb. 2018, https://doi.org/10.1016/j.measurement.2017.10.023.

[11] G. S. Ogato, A. Bantider, K. Abebe, and D. Geneletti, "Geographic information system (GIS)-Based multicriteria analysis of flooding hazard and risk in Ambo Town and its watershed, West shoa zone, oromia regional State, Ethiopia," *Journal of Hydrology: Regional Studies*, vol. 27, Feb. 2020, Art. no. 100659, https://doi.org/10.1016/j.ejrh.2019.100659.

[12] M. Zeleňáková, R. Fijko, S. Labant, E. Weiss, G. Markovič, and R. Weiss, "Flood risk modelling of the Slatvinec stream in Kružlov village, Slovakia," *Journal of Cleaner Production*, vol. 212, pp. 109–118, Mar. 2019, https://doi.org/10.1016/j.jclepro.2018.12.008.

[13] G. Brunner, *HEC-RAS 2D River Analysis System User's Manual*, Hydrologic Engineering Center, 2024.